High-Resolution Studies of the Solar Polar Magnetic Fields

J. R. Varsik
Big Bear Solar Observatory/New Jersey Institute of Technology
40386 North Shore Lane, Big Bear City, CA 92314

P. R. Wilson and Y. Li
University of Sydney
School of Mathematics and Statistics,
Sydney, NSW 2006

(Received ..... ; Accepted in final form .....)

Abstract. We present high-resolution studies of the solar polar magnetic fields near sunspot maximum in 1989 and towards sunspot minimum in 1995. We show that, in 1989, the polar latitudes were covered by several unipolar regions of both polarities. In 1995, however, after the polar field reversal was complete, each pole exhibited only one dominant polarity region.

Each unipolar region contains magnetic knots of both polarities but the number count of the knots of the dominant polarity exceeds that of the opposite polarity by a ratio of order 4:1, and it is rare to find opposite polarity pairs, i.e. magnetic bipoles.

These knots have lifetimes greater than 7 hours but less than 24 hours. We interpret the longitudinal displacement of the knots over a 7 hour period as a measure of the local rotation rate. This rotation rate is found to be generally consistent with Snodgrass' (1983) magnetic rotation law.

In an attempt to obtain some insight into the operation of the solar dynamo, sketches of postulated subsurface field configurations corresponding to the observed surface fields at these two epochs of the solar cycle are presented.

1. Introduction

The direct measurement of the splitting of a Zeeman-sensitive spectral line by the magnetic field of a sunspot, as measured by G.E. Hale in 1908 (Hale and Nicolson 1938) opened a new era in solar physics, the 'Mt. Wilson era'. The development of the photoelectric magnetograph by H.D. and H.W. Babcock (Babcock, H.D. and Babcock, H.W. 1952) and the improvements which have been made to this and other instruments during the past three decades (e.g. Beckers and Schroter 1968, Harvey 1977) have permitted high-resolution studies of the fine structure of the solar magnetic fields. Reviews of this early work have been provided by Severny (1972), Howard (1977, and Zwaan (1987).

In these studies it was shown that the general magnetic field of the Sun consists of small (1-2 arcsec), intense ($\sim$ 1200 G) flux knots of mixed polarities. In high-resolution magnetograms in which positive fields are indicated by white and negative by black, these regions are sometimes described as 'pepper and salt' regions because the flux knots of both polarities are fairly evenly distributed. In other regions, however, the knots of one polarity are seen to dominate over the other, and Severny shows that, at low resolution, the knots of the dominant polarity tend to mask those of the opposite polarity, the region being often described as a 'unipolar' region. A region defined by the neutral lines of the large-scale field seen at low resolution, as given either by the zero level of a contour plot of the magnetic field or as inferred from filaments seen in Hα spectroheliograms, is sometimes called a 'magnetic cell' and is generally cospatial with a unipolar region.

During most of the cycle the polar regions are occupied by unipolar magnetic cells of opposite polarities and, following Babcock's observation of the reversal of the polar fields in 1954, Severny reported the change of the magnetic polarities at both poles in 1964-65, noting that the changes were not simultaneous. Recent high-resolution studies of the polar fields (Lin, Varsik, and Zirin, 1993) show that, like the fields at lower latitudes, the polar magnetic fields are concentrated into small magnetic elements of both polarities. Although the polar regions may appear as unipolar in low-resolution magnetograms, these observations show that, within those regions, magnetic elements of both polarities are present and that one polarity tend to dominate the other.

As the cycle progresses, the predominant polarity in each hemisphere changes and Fox, McIntosh, and Wilson (1997) have described the evolution of the large-scale fields and their association with coronal holes during the polar field reversals. This study shows that the dominant processes take place on a global rather than a local scale. The present studies are intended to complement that work by investigating the evolution of the small scale structures of which the large-scale unipolar regions are composed.

It is generally agreed that the imperatives of Maxwell's equations, in particular

$$\nabla \cdot B = 0, \tag{1}$$

require that magnetic fields observed at the solar surface must be connected either above or below the surface. While many writers have described the coronal connections, based on Hα and X-Ray observations or on potential field calculations (see e.g. Wilson 1994, p 57), few have been sufficiently brave (or foolhardy) to attempt to describe the subsurface connections. Nevertheless, if we are to obtain some guidelines from observation as to the nature of the solar dynamo, some descriptions must be attempted. In this paper, further studies of the small-scale and large-scale polar magnetic fields at the Big Bear Solar

Observatory (BBSO) in 1989 and 1995 (i.e. near sunspot maximum and minimum) are reported and an attempt is made to sketch the subsurface field configurations corresponding to the observed surface fields at these two epochs of the solar cycle.

2. The Data

High-resolution magnetograms of the solar polar regions have been obtained at BBSO during the periods June 19-July 10, 1989, i.e. Carrington rotation (CR) 1817 and June 14-July 10, 1995, (Carrington rotation 1897). The pixel scale is about 0.6 arcsec/pixel and the seeing was of the order of 2 arcsec on the best images. Each magnetogram image is approximately 300 x 225 arcseconds in size.

Individual magnetograms have been combined to yield mosaics of the polar region. For 1995, each mosaic (see Figure 3 for examples) consisted of four overlapping images, three containing the solar limb and one centered on the central meridian and overlapping with the central limb image. The 1989 mosaics consist of sets of seven or eight similar-sized magnetogram images, with four or five images including the limb and other images centerward of, but overlapping with, the limb images. Examples can be found in Figure 1. Two polar mosaics (north and south) were acquired in the morning and two in the afternoon of each day.

A high-pass filter was applied to these data to remove nonuniformities introduced by the KDP crystal. In the 1989 data in particular this also has the effect of introducing "halos" of apparent opposite polarity around magnetic field elements. These are artifacts and should be ignored. In order to correct for guider errors and telescope flexure the position of the limb was found using a Sobel filter on the intensity images that were obtained at the same time as the magnetograms. This, along with the known image scale, allowed the actual position of the telescope on the Sun to be determined. Images that did not contain any component of the limb were overlapped with limb-included images, their positions and orientations being determined by matching positions of magnetic features on both images.

Figure 1 depicts mosaics of the polar fields for July 9, 1989 (i.e. within Carrington rotation 1817). Although the field-strengths for the 1989 magnetograms are not accurately calibrated, the magnetic polarities of the features are correctly assigned. Reference grids have been superimposed on these mosaics, indicating the solar latitude and longitude with respect to the central meridian. The magnetic fields appear in the form of flux knots of one or other polarity but, within the mosaic, at

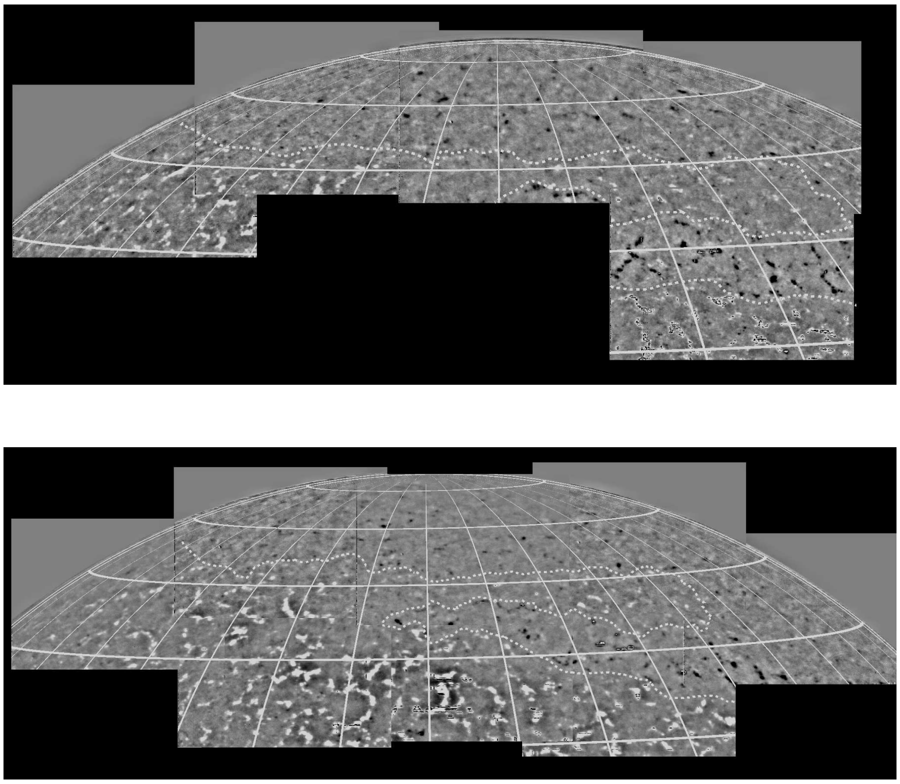

Figure 1. Mosaics of BBSO magnetograms for July 9, 1989 (CR 1817). North pole shown, along with boundaries of unipolar regions (indicated by the dashed curves). The upper image is from 15:50 UT, while the lower is from 23:40 UT. The magnetic knots are seen as concentrations of magnetic flux. The solid lines are spaced at 10° intervals in heliographic latitude and longitude. In addition a line is drawn at the estimated position of the solar limb as well as one three arcseconds in from the limb.

least two distinct regions may be delineated within which the number of knots of one polarity exceeds that of opposite polarity by a ratio of order 4:1.

McIntosh has used the locations of Hα filaments to chart the neutral lines of the large-scale fields and his synoptic chart for CR 1817 is shown in Figure 2. By plotting the high-latitude north-polar neutral line from this chart on to the high-resolution magnetogram for this date, it is clear that the regions of one predominant polarity identified in Figure 1 are simply the large-scale unipolar regions as shown on the synoptic charts.

In Figure 3(a), similar mosaics have been constructed, showing the north polar magnetic fields on June 20, 1995, (a) at 17:00 UT, and

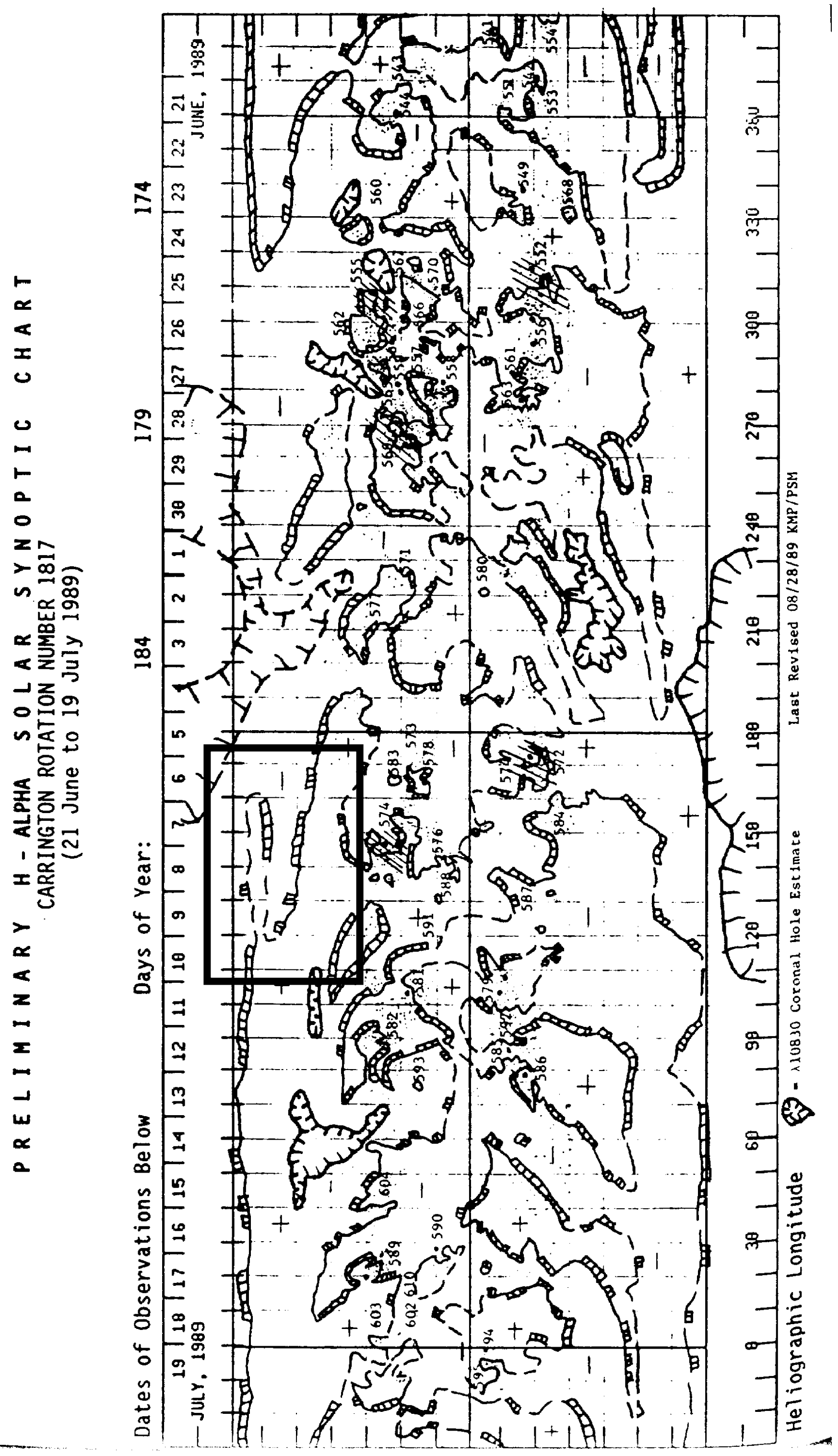

Figure 2. McIntosh Hα synoptic chart (1989, *Solar-Geophysical Data*, #541, 48) for CR 1817. The positive polarity feature at latitude 55°N, Carrington longitude 140° (enclosed by a box) corresponds to the feature seen in Figure 1.

(b) at 24:00 UT. The numbers indicate the positions of the magnetic knots used as tracers of the solar rotation, and are the same as the ID numbers in Table 1. Again reference grids have been superimposed on these magnetograms, which have been calibrated according to a method described by Varsik (1995). Here the longitudes are measured in respect to the central meridian which, at the former time, corresponded to a Carrington longitude of 256.5°. In Figure 3(b), similar mosaics are shown for the south polar region.

3. Results

From these and other mosaics we have studied, the following general results may be derived:

1. In both 1989 and 1995 it can be seen that the large unipolar regions observed in low-resolution magnetograms consist of predominantly isolated knots of magnetic field of either polarity. These knots average about 7.3 Mm diameter and appear to form part of the magnetic network which is believed to lie along the edges of supergranule cells. They have a magnetic flux of about 1×10^{19}Mx, based on the calibrated 1995 magnetograms.

2. In a unipolar region of given polarity, the numbers of magnetic knots of that polarity exceed those of the opposite polarity by a ratio of order 4:1, although we emphasize that this value is very uncertain, being very sensitive to spatial resolution and signal sensitivity. However we have used numbers of knots rather than flux-strengths in order to relate these observations to the models of the subsurface fields illustrated the sketches shown in Figures 7 and 8.

3. In any given image, some patterns or collections of knots of the dominant polarity may be seen and, while these knots can often be recognized after an approximately 7 hour period, they can only rarely be followed from one day to the next.

4. Only a small numbers of bipoles are found with footpoints comparable in strength with the magnetic knots which form the network. Bipoles may be identified as adjacent regions of positive and negative flux and are perhaps connected either above or below the surface. Some care must be exercised since, near the limb, apparent bipoles may appear as a result of the divergence of a single knot of flux. Only opposite polarity pairs near the central meridian with magnetic axis oriented (approximately) in the longitudinal (i.e. east-west) direction are likely to be genuine bipoles and, as can be seen from Figures 1 and 3, these are not common.

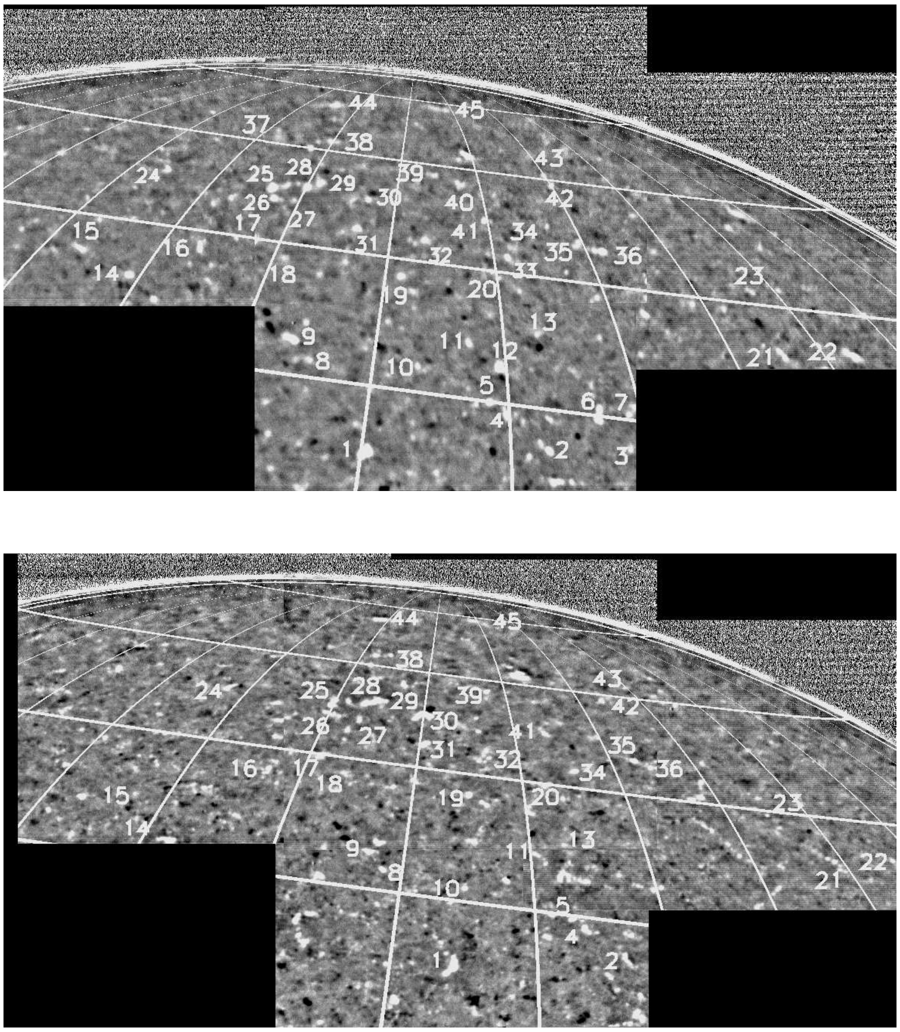

Figure 3a. Mosaics of BBSO magnetograms, June 20, 1995, 17:00 and 24:00 UT, for the north solar pole. The numbers indicate the positions of the magnetic knots used as tracers of the solar rotation, and are the same as the ID numbers in Table 1.

5. Where patterns of magnetic knots can be recognized after ~7 hours, their longitudinal displacements during the 7 hour period may be expressed in terms of rotation rates as a function of latitude. These rates, derived from several image pairs in 1989 and 1995, are plotted in Figures 4 and 5, and may be compared with the magnetic rotation law derived by Snodgrass (1983) for somewhat larger magnetic regions (see below).

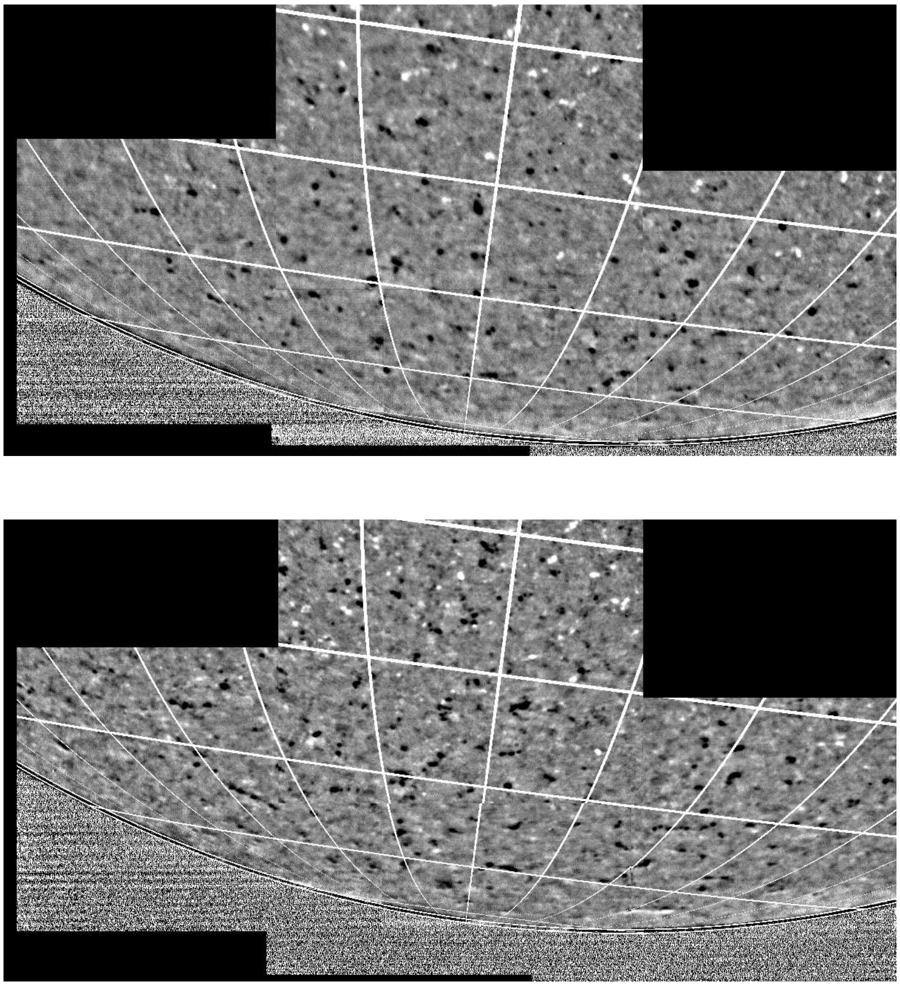

Figure 3b. Mosaics of BBSO magnetograms, June 20, 1995, 17:00 and 24:00 UT, for the south solar pole.

6. By contrast to the polar regions of 1995, which were each covered by single magnetic cell of one dominant polarity, the corresponding regions of 1989 exhibited several smaller unipolar regions of both polarities. Thus the unipolar regions, rather than the individual magnetic features, appear to be the dominant identifiable phenomena.

7. The apparent lack of interaction between these knots and the infrequency of bipole-like pairings, suggest that the evolution of the flux-knot patterns is not determined by surface phenomena, such as meridional motions, but arise from sub-surface 'flux-trees' which evolve continuously. Some examples are sketched in Figures 7 and 8.

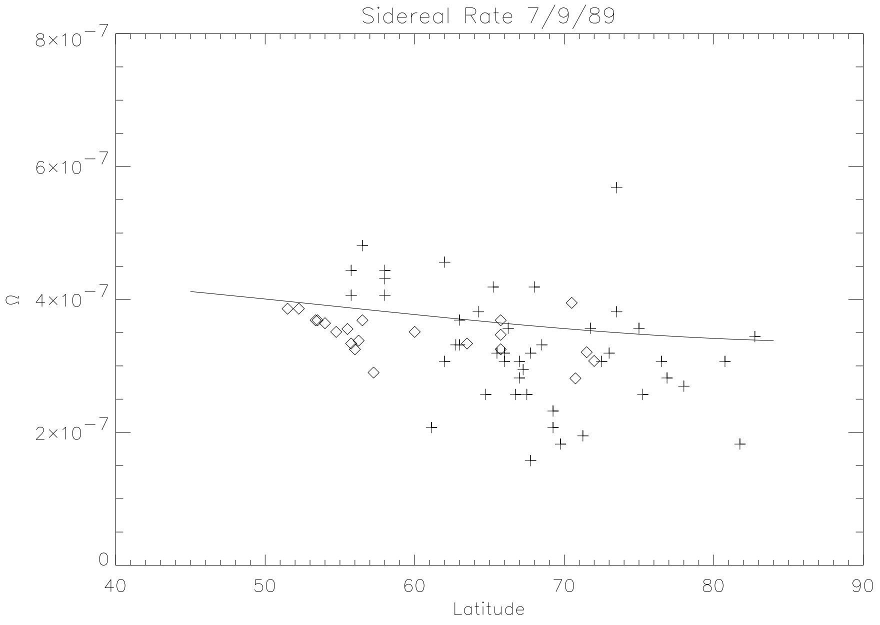

Figure 4. Rotation rate, July 9, 1989, north and south poles. The north pole knots are shown as plus signs; the south pole knots are shown as diamonds. The curve is that of Snodgrass (1983).

4. The Polar Rotation Rate

By remapping the polar images of Figures 1 and 3 on to a rectangular coordinate system, the longitudinal displacements of recognizable patterns of knots may be measured over a time-interval of ~ 7 hr. In Figure 3a, the selected knot patterns for the north pole are indicated by numbers, and the mean latitudes and initial Carrington longitudes for these points are shown in Table 1. The longitudinal displacements relative to the central meridian during the ~ 7 hour period are also shown in Table 1 and, using the precise time intervals, these are expressed in terms of rotation frequencies (in nHz).

These 'rotation rates' are plotted against latitude in Figure 4 for the northern and southern hemispheres on July 9, 1989, and in Figure 5 for June 22, 1995. where they may be compared with Snodgrass' (1983) magnetic rotation law,

$$\frac{\Omega}{2\pi}(\lambda) = 462 - 74\mu^2 - 52\mu^4, \tag{2}$$

where λ is the latitude and $\mu = \sin\lambda$. In Figure 6, all the data points for both hemispheres and for both years of observation have been plotted

Table I. Latitude and displacement of knots observed in the north polar region on June 20, 1995. The ID numbers are the same as those in Figure 3a.

ID	C. Long.	Lat.	Δ Long.	Ω (nHz)
1	256.2	45.5	3.67	456.5
2	268.5	47.1	3.54	442.0
4	265.6	49.1	3.67	456.5
5	264.4	49.9	4.04	500.0
8	251.2	51.1	3.04	384.1
9	249.6	52.4	3.30	413.1
10	259.1	51.8	4.42	543.3
11	263.0	53.9	4.92	601.1
13	268.1	55.2	2.54	326.2
14	235.0	55.4	3.54	442.0
15	229.2	57.0	3.80	470.9
16	239.2	58.4	3.42	427.5
17	244.2	59.9	2.67	340.7
18	246.9	58.6	2.42	311.8
19	257.2	58.5	3.54	442.0
20	266.1	59.2	2.67	340.7
21	291.2	55.9	3.54	442.0
22	299.6	56.6	2.54	326.2
23	292.6	60.9	3.17	398.6
24	229.9	65.2	3.42	427.5
25	242.5	64.9	3.04	384.1
26	243.2	63.9	3.17	398.6
27	245.4	63.9	3.80	470.9
28	246.0	65.5	3.04	384.1
29	247.1	66.0	3.54	442.0
30	253.0	65.1	3.30	413.1
31	252.6	62.1	3.54	442.0
32	259.2	61.9	2.54	326.2
34	267.6	62.1	3.67	456.5
35	275.5	63.5	3.17	398.6
36	277.8	63.0	2.30	297.3
38	245.8	71.1	2.54	326.2
39	260.1	68.8	3.17	398.6
41	265.5	64.4	3.80	470.9
42	275.8	69.1	3.67	456.5
43	275.8	70.4	3.92	485.4
44	241.2	76.6	2.80	355.2
45	262.4	78.6	3.42	427.5

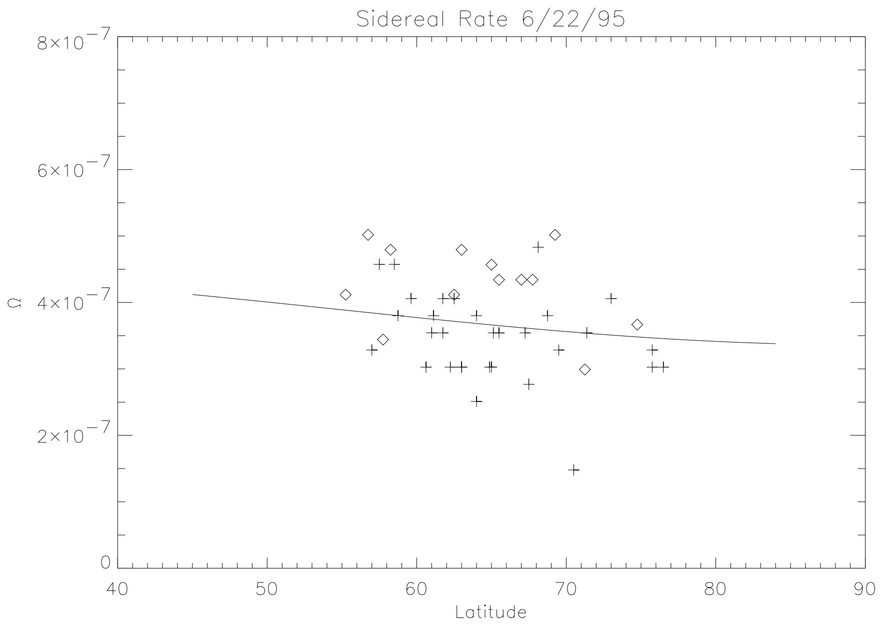

Figure 5. Rotation rate, June 22, 1995, north and south poles. The north pole knots are shown as plus signs; the south pole knots are shown as diamonds. The curve is that of Snodgrass (1983). We note that the north pole rotation rate appears slower than the south pole rotation rate. However, the scatter in the data (particularly at the north pole) is large. This difference in the rotation rate may be an interesting result if it can be confirmed using other 1995 data. This investigation is in progress.

together with curves representing (a) a least squares fit to these points and (b) the Snodgrass rotation law.

These plots, particularly the latter, exhibit a degree of scatter exceeding that which might have been expected from measurement error and it may be noticed that the scatter increases from latitude 50° to 70°, which is qualitatively consistent with random motions associated with the supergranulation. The curve derived from Equation (2) lies well within the 1-σ uncertainty interval drawn about the least squares curve (indicated by the dashed lines). Thus, while there is some tendency to follow a latitude dependent rotation law, these observations require a considerable random motions to be superimposed on this law.

The scatter is as yet too large to allow any conclusions to be drawn about any possible solar cycle variation of the high-latitude rotation rate of magnetic knots (as has been suggested by Komm *et al.* 1992).

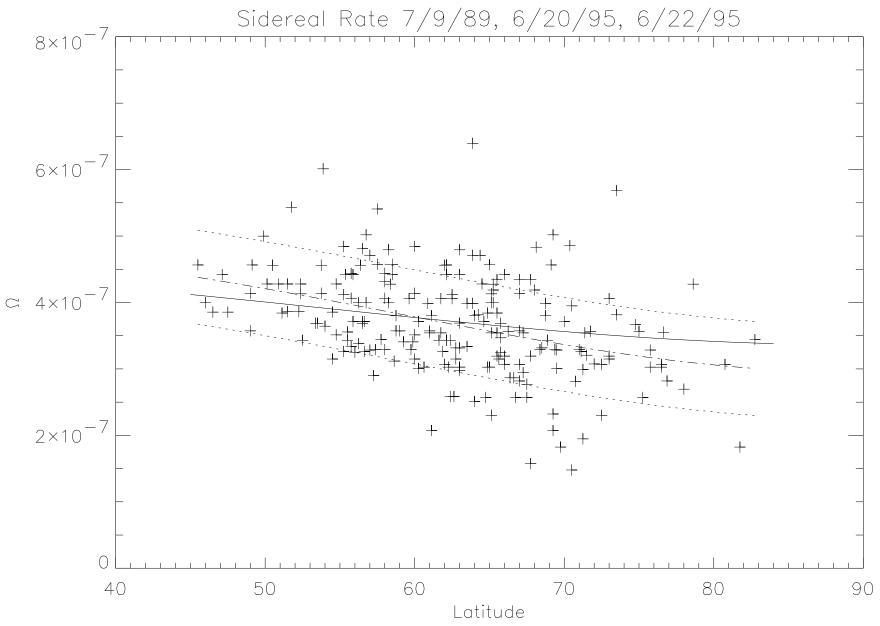

Figure 6. Combined rotation rate data for July 9, 1989 and June 20 and 22, 1995. The solid curve is the Snodgrass rotation rate. The dashed curve is a least-squares fit to the data, using a rotation law of the same form as the Snodgrass law. The dotted lines indicate the $\pm 1\sigma$ uncertainty interval around the fitted curve.

5. Discussion

These results raise the basic questions:

1. What is the mechanism (or mechanisms) that generates these magnetic knots?

2. How are these knots organized into large unipolar regions so that they exhibit polarity ratios of order 4:1 within these regions?

3. What causes the difference in the configurations observed in 1989 and 1995?

The structure of these unipolar regions, in particular the scarcity of obvious bipole structures, suggests that they are generated by some more global subsurface mechanism rather than by the random emergence of small bipoles. While it would be helpful to be able to compute the sub-surface field structures on the basis of the observed surface fields (as may be done for coronal field structures by assuming that the fields are potential) this is simply not possible for the sub-surface fields. Nevertheless the absence of magnetic monopoles and the constraints imposed by equation (1) require that the surface fields must delineate the surface intersections of field lines which thread the interior and re-emerge at some other location marked by flux knots of opposite polarity. Therefore we believe that some insight into the subsurface field structures may be gained by attempting to draw the simplest system of subsurface field lines consistent with the observed surface fields and with Equation (1).

This process has sometimes been criticized as 'cartoon astrophysics' but, while we would agree that the fieldlines which we construct are little more than educated guesses, we know of no other way of attempting to understand the subsurface fields on this scale.

Snodgrass and Wilson (1992) described how a subsurface Ω-loop may emerge through the surface layers, giving rise first to bipoles with a preferred orientation and then, via reconnections, to the large scale unipolar regions in which one polarity is dominant. Wilson, McIntosh, and Snodgrass (1990) showed how such an Ω-loop may be sheared, and then repaired to form a U-loop (their Figure 1(c), here reproduced as Figure 7(a)), and this may be compared with Figure 3 of Giovanelli (1985). In Figure 7(b) we extend this picture of a closed U-loop to show how a unipolar region, represented in this figure by diagonal hatching, may indeed consist of flux knots of both polarities, here shown in the ratio 4:1, some of the knots of the dominant polarity being connected below the surface through the branches of a *flux-tree* (see e.g. Piddington, 1981) to deeply rooted poloidal field lines and above by coronal field loops, while adjacent knots of both polarities may be related to simple bipoles. Here the field lines which extend above the surface are represented by solid lines and the subsurface field lines by broken lines. This concept is now applied to represent the subsurface structure of the polar fields in 1989 and 1995 as described above.

In Figure 8 we sketch (in idealized form) the above-surface field lines (full lines) which may be typical of the polar fields in (i) 1995, when the polar region is of a single unipolar polarity, and (ii) 1989 when several unipolar regions of both polarities are seen. The fields are represented by a mixture of the foot-points of coronal arches and small bipolar loops and the dashed lines indicate the assumed surface neutral lines of the large-scale fields, the corresponding unipolar regions being shaded with a forward-inclined slant for a positive region and a backward-inclined slant for a negative region. Again the ratio of knots of opposite polarities within these regions is 4:1, which is of the same order as that reported above. Coronal holes are indicated by a 'crown'.

Following Figure 7(b), we show by dotted lines a possible configuration for the sub-surface fields which is consistent with the surface fields.

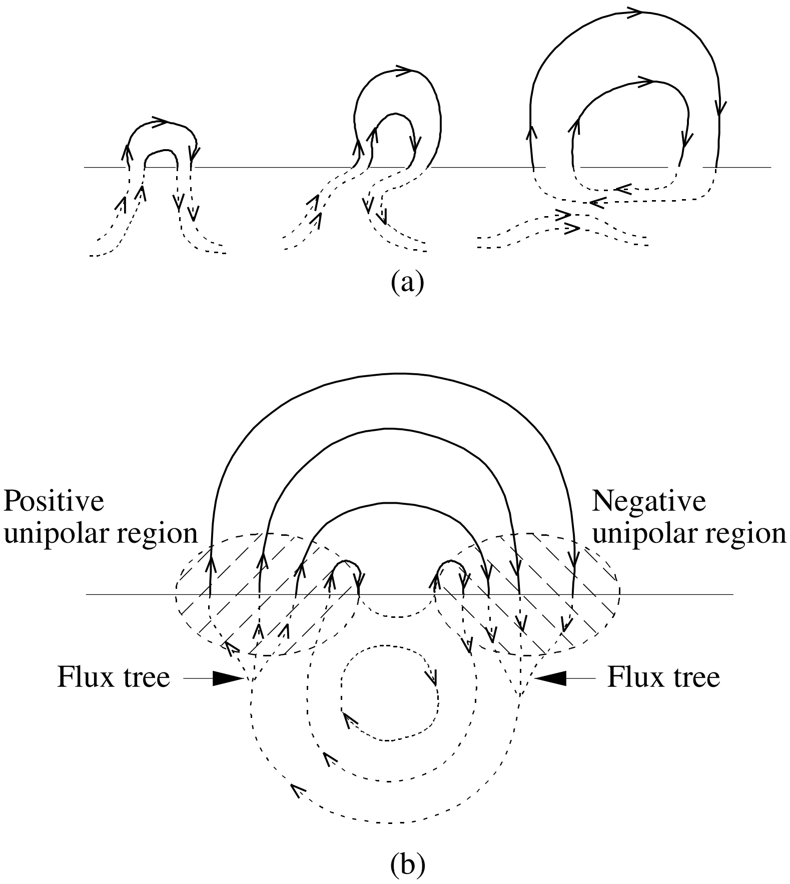

Figure 7. Here is shown (a) how an Ω-loop may be repaired (following Spruit *et al.*) to yield a sub-surface U-loop with fieldline connections in the form of coronal loops. In (b) is shown a possible subsurface field configuration consistent with two large-scale unipolar regions within which the ratios of flux-knots of opposite polarities are 4:1 and 1:4. The branching of the sub-surface field-lines into flux-trees is illustrated.

6. Conclusion

In this paper we have extended the ideas of Snodgrass and Wilson (1992) to explain our high-resolution observations of the solar polar magnetic fields. We have shown that they are consistent with the organization of magnetic knots by subsurface fields. We also have measured the rotation rate of these magnetic knots and found it to be consistent with that of the larger regions observed by Snodgrass (1983).

We have postulated the presence of a subsurface field structure that is consistent with the observed surface poloidal fields at sunspot minimum when the polar fields are strongest and at sunspot maximum

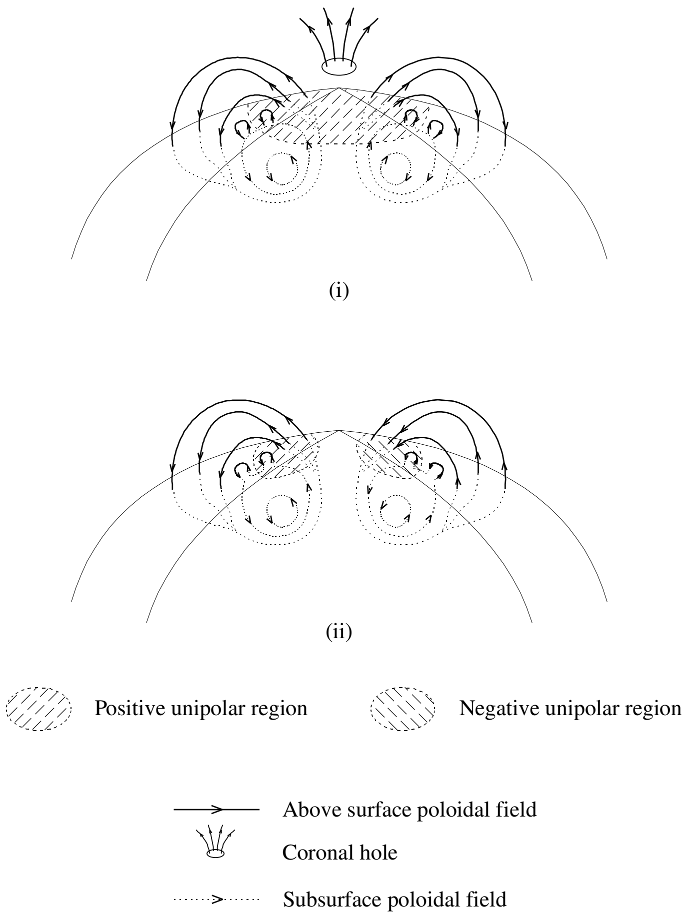

Figure 8. In this figure the full lines illustrate, in idealized form, the above-surface field-lines in the polar region when (i) the polar region is covered with a unipolar region, as in the observations for 1995 shown above. In this region the flux knots of the dominant polarity exceed those of opposite polarity in the ratio 4:1. In (ii) the polar region is covered by large-scale regions within which one or other polarity is dominant, as in the case of the polar regions as observed in 1989 (above). The dotted lines illustrate a possible sub-surface field configuration which may correspond to the above-surface fields.

when they are about to reverse. This raises the question as to whether these fields arise in response to a local polar dynamo and, if so, how it is related to the dynamo that generates the active region magnetic fields. Similar questions have been raised by Legrande and Simon (1981), and by Fox, McIntosh, and Wilson (1998), and will be pursued in a later paper.

Acknowledgements

We wish to acknowledge the help of the BBSO observers in obtaining the polar magnetograms.

PRW thanks the BBSO and the National Solar Observatory at Sunspot for their hospitality from time to time during this project and acknowledges the support of the Australian Research Council through Grant A69131266.

References

Babcock, H.W., and Babcock, H.D.: 1955 *Astrophys. J.*, **121**, 349.
Beckers, J. M., and Schroter, E.H.: 1968, *Solar Physics*, **4**, 142.
DeVore, C. R., Sheeley, N. R., and Boris, J. P.: 1984, *Solar Physics*, **92**, 1.
DeVore, C. R., and Sheeley, N. R.: 1987, *Solar Physics*, **108**, 47.
Fox, P., McIntosh, P., and Wilson, P. R.: 1998, *Solar Physics* **171**, 375.
Giovanelli, R.G.: 1985, *Australian J. Phys.*, **38**, 1045.
Harvey, J.W.: 1977, *Highlights in Astronomy* ed Edith A. Muller, **4(2)** , 223.
Howard, R.F.: 1977, *Ann. Rev. Astron. Astrophys.* **15**, 153.
Komm, R. W., Howard, R. F., Harvey, J. W., and Forgach, S.: 1992, in K. L. Harvey (ed.), *Proceedings of the National Solar Observatory/Sacramento Peak 12th Summer Workshop*, San Francisco, California, p. 325.
Legrand, J.P., and Simon, P.A.: 1981, *Solar Phys.* **70**, 173.
Leighton, R. B.: 1964, *Astrophys. J.*, **140**, 1547.
Lin, H., Varsik, J. R., and Zirin, H.: 1993, *Solar Physics*, **155**, 243.
McIntosh, P.S.: 1992, in K. L. Harvey (ed.), *Proceedings of the National Solar Observatory/Sacramento Peak 12th Summer Workshop*, San Francisco, California, p. 14.
Murray, N., and Wilson, P. R.: 1992, *Solar Physics*, **142**, 221.
Piddington, J.H.: (1981), *Cosmic Electrodynamics* Krieger, Florida, (2nd edit), p116.
Severny, A.: 1972, *Vistas in Astronomy*, **13**,135.
Sheeley, N. R., Nash, A. G., and Wang, Y.-M.: 1987, *Astrophys. J.*, **319**, 481.
Snodgrass, H. B.: 1983, *Astrophys. J.*, **270**, 288.
Snodgrass, H. B., and Wilson, P. R.: 1993, *Solar Physics*, **148**, 179.
Spruit, H. C., Title, A. M., and van Ballegooijen, A. A.: 1987, *Solar Physics*, **110**, 115.
Stenflo, J. O.: 1992, in K. L. Harvey (ed.), *Proceedings of the National Solar Observatory/Sacramento Peak 12th Summer Workshop*, San Francisco, California, 83.
Varsik, J. R.: 1995, *Solar Physics*, **161**, 207.
Wang, Y.-M., Nash, A. G., and Sheeley, N. R.: 1989, *Science*, **245**, 861.
Wilson, P. R.: 1994, *Solar and Stellar Activity Cycles*; Cambridge Astrophysics Series No. 24, Cambridge University Press.

Wilson, P. R., and Giovannis, J.: 1994, *Solar Physics*, **155**, 29.
Wilson, P. R., McIntosh, P. S., and Snodgrass, H. B.: 1990, *Solar Physics*, **127**, 1.
Zwaan, C.: 1987, *Ann. Rev. Astron. Astrophys*, **25**, 89.